Science of the Total Environment 903 (2023) 166191

Contents lists available at ScienceDirect

Science of the Total Environment

journal homepage: www.elsevier.com/locate/scitotenv

Source apportionment and ozone formation mechanism of VOCs considering photochemical loss in Guangzhou, China

Y. Zou [a,b], X.L. Yan [c], R.M. Flores [d], L.Y. Zhang [b], S.P. Yang [b], L.Y. Fan [a], T. Deng [b], X.J. Deng [b], D.Q. Ye [a,*]

[a] School of Environment and Energy, South China University of Technology, Guangzhou 510006, China
[b] Institute of Tropical and Marine Meteorology, China Meteorological Administration (CMA), Guangzhou 510640, China
[c] State Key Laboratory of Severe Weather & Institute of Tibetan Plateau Meteorology, Chinese Academy of Meteorological Sciences, Beijing, China
[d] Marmara University, Department of Environmental Engineering, Istanbul, Turkey

HIGHLIGHTS

- Approximately 17 % of the initial concentration of VOCs was lost during transport.
- Five types of VOC sources were identified and quantified in the summer and autumn.
- Alkenes and aromatics accounted for more than 80 % of the OFP loss of total VOCs.
- Consideration of chemical loss resulted in less control of VOCs in ozone formation.

GRAPHICAL ABSTRACT

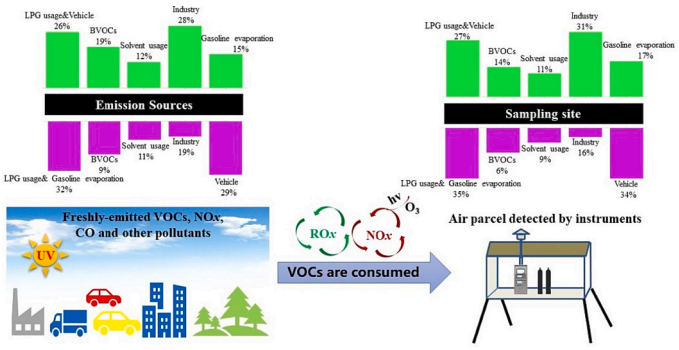

ARTICLE INFO

Editor: Jianmin Chen

Keywords:
Volatile organic compounds (VOCs)
Photochemical age
Ozone pollution
Megacity

ABSTRACT

Understanding the sources and impact of volatile organic compounds (VOCs) on ozone formation is challenging when the traditional method does not account for their photochemical loss. In this study, online monitoring of 56 VOCs was carried out in summer and autumn during high ozone pollution episodes. The photochemical age method was used to evaluate the atmospheric chemical loss of VOCs and to analyze the effects on characteristics, sources, and ozone formation of VOC components. The initial concentrations during daytime were 5.12 ppbv and 4.49 ppbv higher than the observed concentrations in the summer and autumn, respectively. The positive matrix factorization (PMF) model identified 5 major emission sources. However, the omission of the chemical loss of VOCs led to underestimating the contributions of sources associated with highly reactive VOC components, such as those produced by biogenic emissions and solvent usage. Conversely it resulted in overestimating the contributions from VOC components with lower chemical activity such as liquefied petroleum gas (LPG) usage, vehicle emissions, and gasoline evaporation. Furthermore, the estimation of ozone formation may be underestimated when the atmospheric photochemical loss is not taken into account. The ozone formation potential (OFP) method and propylene-equivalent concentration method both underestimated ozone formation by 53.24 ppbv and 47.25 ppbc, respectively, in the summer, and by 40.34 ppbv and 26.37 ppbc, respectively, in the

* Corresponding author.
E-mail address: cedqye@scut.edu.cn (D.Q. Ye).

https://doi.org/10.1016/j.scitotenv.2023.166191
Received 10 April 2023; Received in revised form 7 August 2023; Accepted 8 August 2023
Available online 9 August 2023

autumn. The determination of the ozone formation regime based on VOC chemical loss was more acceptable. In the summer, the ozone formation regime changed from the VOC-limited regime to the VOC-NO*x* transition regime, while in the autumn, the ozone formation regime changed from the strong VOC-limited regime to the weak VOC-limited regime. To obtain more thorough and precise conclusions, further monitoring and analysis studies will be conducted in the near future on a wider variety of VOC species such as oxygenated VOCs (OVOCs).

1. Introduction

With the development of the economy and urbanization, the Pearl River Delta (PRD) region has experienced persistently high levels of air pollution emissions, leading to a decline in air quality. One of the main concerns is the increasing ozone pollution, which hampers efforts to improve the region's air quality. Therefore, it is essential to focus on ozone pollution prevention and control [Zou et al., 2015; Yin et al., 2019; Zou et al., 2019a; Li et al., 2022]. Volatile organic compounds (VOCs) play a significant role in the formation of secondary pollutants in the atmosphere. The formation of ozone in PRD cities is a chemical reaction process dominated by VOCs. Over the last few decades, extensive research has been conducted examining the characteristics of VOC concentration levels, sources, atmospheric chemical activity, and the nonlinear relationships they exhibit with regard to ozone formation [Guo et al., 2017; Wang et al., 2021; Zou et al., 2021; Wang et al., 2022; Song et al., 2022; Mu et al., 2023].

However, owing to the high reactivity and abundance of VOC species in the atmosphere, they undergo a series of photochemical reactions during their transport from emission sources to receptor sites, resulting in different degrees of chemical loss. Therefore, traditional analyses and research relying on VOC data collected at observation sites have encountered challenges in the past. This is primarily because VOCs observed at receptor sites differ from those emitted by sources in terms of their concentrations, compositional characteristics, atmospheric chemical activity, and mechanisms of ozone formation. Firstly, regarding the concentration and composition of VOCs, Zhan et al. (2021) found that alkenes (43.8 %) and aromatics (18.1 %) emitted in Beijing during the summer were lost due to photochemical reactions occurring during transport. Gao et al. (2021) conducted observational studies in an industrial area and found high concentrations of reactive VOC species (e.g., alkenes) with high chemical losses. Secondly, when conducting source analyses of VOCs, it is crucial to consider the underlying assumptions of receptor models, such as positive matrix factorization (PMF) and chemical mass balance (CMB). These models rely on the assumption that the species composition of VOCs at the receptor site remains unchanged from that of the source emissions, disregarding any photochemical reactions occurring in the atmosphere. However, in reality, photochemical reactions do take place, leading to transformations in the VOC composition at the receptor site. For example, Na and Kim (2007) and Bon et al. (2011) found significant differences between the chemical loss of VOCs determined through transmission and the loss estimated from data measured at the observation site. They also found that source analysis without considering the chemical loss of VOCs underestimates the contribution of emission sources. Finally, regarding the OFP (ozone formation potential) and mechanisms associated with VOCs, previous estimations did not account for the chemical loss of VOCs. Consequently, a study by Wang et al. (2013) demonstrated that the OFP of 56 VOCs in the Shanghai area had been severely underestimated by 60 %. Similarly, Zhan et al. (2021) found that the ozone formation regime would move from VOC-limited regime to VOC-NO*x* transition regime or NO*x*-limited regime after considering the chemical loss of VOCs. Given that ozone formation is associated with the chemical loss of VOCs, this approach is more reasonable than solely relaying on observation data to determine the ozone formation regime. To develop efficient control strategies and emission reduction measures for atmospheric photochemical O_3 pollution, it is crucial to evaluate the chemical loss of VOCs. OH radicals are important oxidants in the atmosphere, dominating the oxidative removal of VOC species and playing a key role in the formation of O_3 [Atkinson and Arey, 2003; Shao et al., 2009]. Many researchers have conducted VOC chemical loss correlation analyses using the photochemical age method in China's large cities, such as Beijing, Shanghai, and Taiwan, via the consumption formula of OH radical reaction [Shiu et al., 2007; Shao et al., 2011; Wang et al., 2013; Gao et al., 2018; Zhan et al., 2021; Wu et al., 2023]. Additionally, the higher temperatures and intensified radiation during the summer and autumn seasons contribute to stronger photochemical reactions, resulting in a higher degree of chemical loss of VOCs, which leads to increased ozone formation. This factor significantly contributes to the frequent ozone pollution episodes in summer and autumn, characterized by hourly concentrations exceeding 93 ppbv, a threshold defined by a new Chinese ambient air quality standard (GB 3095-2012, 2012) [Yin et al., 2019; Meng et al., 2023]. In order to effectively address the increasing trend of ozone pollution in the PRD, it is crucial to prioritize and strengthen research efforts focused on the Guangzhou area within the PRD , especially during the summer and autumn seasons experiencing high occurrences of ozone pollution.

This study relies on the Urban Eco-Meteorological Comprehensive Observation Base in Haizhu District, Guangzhou to carry out online observations of VOCs during the summer (June, July, and August) and autumn (September, October, and November) with high ozone incidences in the year 2021. It uses the photochemical age-based parameterization method to evaluate the chemical loss of atmospheric VOCs and then analyzes the effect of the atmospheric chemical transformation of VOCs on their compositional characteristics, source analysis, OFP, and ozone formation regime. This study provides a scientific basis for the implementation of comprehensive measures to prevent and control atmospheric photochemical ozone in Guangzhou city.

2. Methodology

2.1. Site description

This study relies on the Urban Eco-Meteorological Comprehensive Observation Base in Haizhu District, Guangzhou (23°05′N, 113°22′E) (Fig. 1) to carry out synchronous online observations of VOCs, NO*x*, O_3, and meteorological variables. The sampling site is located at the Guangzhou Haizhu National Wetland Park. The observation site is in a basic farmland protection area with a typical composite wetland system composed of a mosaic of central sandbanks, rivers, gullies, and fruit forests. It is also surrounded by commercial streets, residences, and traffic arteries. Thus, the site represents a mixture of wetland climate and human activities. The diurnal variation of alkanes, alkenes, alkynes, and aromatics showed a bimodal variation pattern at the monitoring site in the summer and autumn, as shown in Fig. S1. In contrast, isoprene, primarily emitted from biogenic sources, showed a unimodal variation pattern. Throughout these periods, the relative contribution ratios of these compounds remained relatively consistent. This demonstrates that the emitted VOCs are evenly mixed and transported through the atmosphere to the monitoring site, validating the suitability of our monitoring site as appropriate for studying the chemical transformation of VOCs, as well as their component characteristics, sources, and mechanisms of ozone formation.

2.2. Instrumentation

In this study, we monitored VOCs at a 1-h sampling frequency using the GC5000 online gas chromatograph analyzer (AMA Instruments, Germany). This analyzer can automatically sample and continuously measure VOCs (C_2-C_{12}) in the atmosphere. It comprises two subsystems, GC5000VOC and GC5000BTX, along with a DIM200 calibration module and other auxiliary equipment. The analyzer can detect VOCs with boiling points below 200 °C, including low-boiling VOCs in the range of C_2-C_6 and high-boiling VOCs in the range of C_6 —C_{12} totaling 56 species, consisting of 29 alkanes, 11 alkenes + alkynes, and 16 aromatics. To ensure data accuracy, the instrument was calibrated using a five-point method with PAMS (Photochemical Assessment Monitoring Stations), a standard photochemical gas for ozone precursors recognized by the US Environmental Protection Agency (EPA). The standard gas consists of 56 VOCs with a concentration (volume fraction) of 1×10^{-6}. Calibration results indicate that the method detection limit and linear correlation coefficient of each VOC species range from 0.005 ppbv to 0.06 ppbv, and between 0.964 and 0.999, respectively (as shown in Table S1). To address qualitative and quantitative bias caused by peak window drift during the operation of the chromatographic instrument, single-point calibration and peak window drift calibration were regularly performed. Additionally, online spectral chromatography software was used for data processing. Subsequently, the data was checked according to the EPA-recommended methods by Main et al. (1999). Data exceeding 20 % of all VOCs or 3 standard deviations above the mean for a specific species were flagged as anomalous if no suitable explanatory reason could be found after further inspection. Through this inspection method, approximately 12 % of outliers were eliminated to ensure the validity and reliability of subsequent data analysis. Atmospheric ozone was monitored using the Ecotech 9810B (Ecotech Inc. Australia) following the ultraviolet absorption method. Atmospheric NO*x* was monitored using the Ecotech 9841B nitrogen oxide analyzer following the chemiluminescence method. During the reduction of NO_2 to NO through a molybdenum furnace, other nitrogen-containing oxidizing substances may also be reduced to NO, leading to the monitoring value of NO*x* being larger than the actual value [Dunlea et al., 2007; Ran et al., 2011]. Meteorological data, including radiation, wind direction, wind speed, temperature, and pressure, were collected using automatic weather stations.

2.3. Data analysis

2.3.1. Calculation of the initial VOC concentrations

After VOCs are released from the emission source, they are transported through the atmosphere to the monitoring site, and during this transport, they undergo atmospheric photochemical loss. The initial concentration of VOCs refers to the concentration emitted by the source before any photochemical reaction occurs. On the other hand, the observed concentration of VOCs represents the concentration of atmospheric VOCs measured at the receptor site. The VOC chemical loss is the difference between the initial concentration and the observed concentrations. The photochemical age method was employed to estimate the initial concentration of VOCs [Shao et al., 2009]. This method uses the first-order kinetic reaction of VOCs oxidized by OH radicals in the atmosphere for the calculation, as shown below [de Gouw et al., 2005]:

$$[VOCs_i]_0 = \frac{[VOCs_i]_t}{exp(-K_i[OH]\Delta t)} \quad (1)$$

where,$[VOCs_i]_0$ denotes the initial concentration of *the* $VOCs_i$ species at the emission source, $[VOCs_i]_t$ is the observed $VOCs_i$ concentration at the receptor site, K_i is the rate constant for the reaction of $VOCs_i$ with the OH radical, $[OH]$ is the concentration of OH radicals, Δt refers to the photochemical age of the air mass, and $[OH]\Delta t$ is the exposure dose.

The OH exposure dose ($[OH]\Delta t$) is generally calculated using the following formula [Parrish et al., 2007]:

$$[OH]\Delta t = \frac{1}{(K_C - K_B)} \times \left[Ln\left(\frac{[C]}{[B]}|t = t_0\right) - Ln\left(\frac{[C]}{[B]}|t = t\right) \right] \quad (2)$$

B and C are two species of VOCs constituting a species pair. K_B and K_C are the rate constants for the reactions of species B and C with OH radicals, respectively. $\frac{[C]}{[B]}|t = t_0$ refers to the emission ratio of the initial concentrations of species C and B. $\frac{[C]}{[B]}|t = t$ refers to the observed concentration ratio of species C and B at time t. $[OH]$ denotes the concentration of OH radicals, Δt refers to the photochemical age of the air mass, and $[OH]\Delta t$ is the exposure dose.

Notably, to estimate the chemical loss of VOCs using this technique, the following hypotheses must be taken into account:

(1) According to McKeen et al. (1996), the same emission source produces all the main VOC species. Although this assumption may not accurately represent the emission status of all sources, it is generally accepted in related studies [Wang et al., 2013; Gao et al., 2018; Zou et al., 2021; Zhan et al., 2021].

Fig. 1. Monitoring site in Guangzhou – Haizhu station.

(2) The emission of major VOC species is assumed to be fixed, and the impact of new emission sources during the transmission process is considered negligible [Bertman et al., 1995]. As mentioned earlier, the VOC components emitted by different sources are uniformly mixed at the monitoring site. The photochemical ages of the air masses in the summer and autumn in the urban agglomerations of the PRD have been estimated to be approximately 0.71 h and 1.41 h, respectively, with concentrations of OH radicals selected as 1×10^7 molecules·cm^{-3} and 5×10^6 molecules·cm^{-3}, respectively [Yang et al., 2021]. Since most VOC species in the atmosphere have chemical lifetimes lower than 3 h, the impact of long-range transport on the local emission sources is negligible. This finding confirms that the assumption is suitable for the estimation of VOC chemical loss at this monitoring site. However, it is worth noting that Parrish et al. (2007) reported that the assessment of VOC chemical loss becomes uncertain when atmospheric turbulence is severe.

(3) The chemical loss of VOCs during atmospheric transport considers only the reaction with OH radicals, and the influence of NO_3 radicals and sedimentation is considered negligible [Warneke et al., 2007]. Therefore, the photochemical loss time calculated in this study only accounts for the reaction time with the OH radicals. Since the main oxidative removal pathway of VOC species is the daytime reaction with OH radicals [Atkinson and Arey, 2003], this assumption may lead to lower VOC chemical losses than the actual value.

2.3.2. Source apportionment of VOCs

In this study, the PMF5.0 version developed by the US EPA was used to analyze the sources of VOCs. The operating principle of the PMF model is to decompose the sample matrix (nonnegative) into two matrices: the source contribution matrix (G) and source component spectrum matrix (F). Then, a least squares operation is performed to determine the contribution rate and main pollution sources. At the same time, the calculated Q value must be as close to the theoretical Q value as possible. The formula of the model is given as follows:

$$\chi_{ij} = \sum_{k=1}^{p} g_{ik} f_{kj} + e_{ij} \tag{3}$$

where x_{ij} represents the concentration of the *jTh* component in the *iTh* sample; g_{ik} represents the relative contribution of the *kTh* source to the *iTh* sample; f_{kj} represents the content of the *jTh* component in the *kTh* emission source; and e_{ij} is the residual error. *P* represents the number of sources, and for a given value of *p*, the minimum value of the following objective function *Q* is determined to obtain the results of g_{ik} and f_{kj}.

$$Q = \sum_{i=1}^{n} \sum_{j=1}^{m} \left[\frac{\chi_{ij} - \sum_{k=1}^{p} g_{ij} f_{kj}}{\mu_{ij}} \right]^2 \tag{4}$$

where U_{ij} represents the uncertainty of species *j* in sample *I* in each set of raw data; *n* and *m* represent the number of samples and species, respectively, and *p* represents the number of factors. The species samples are treated as an $n \times m$ matrix χ, which is decomposed into an $m \times p$ source contribution matrix G and a $p \times n$ pollution source spectrum matrix F. The PMF receptor model is based on the input VOC data matrix χ by finding the minimum value of the objective function Q to find the source contribution and pollution source spectrum matrix conforming to χ and requiring g_{ik} and f_{kj} to be nonnegative.

PMF typically requires the use of two input matrices: the sample concentration of multiple components and the uncertainty for each component. Uncertainty documents can be obtained from the PMF5.0 User Guide [USEPA, 2014]. The signal-to-noise ratio (S/N) of each species was calculated based on the input file. If 50 % of the samples of the species cannot be detected (<MDL) or its concentration is always below the uncertainty level (S = 0), it cannot be applied for PMF.

2.3.3. The effect of VOCs on photochemical ozone formation

Volatile organic compounds display a broad spectrum of reactivity concerning their contribution to photochemical ozone formation. It is essential to note that their concentrations are not directly proportional to ozone formation, due to the complex interplay between various factors such as composition, atmospheric conditions, and the presence of other species. Maximum incremental reactivity (MIR) factor and OH radical reactivity are two main methods used to evaluate the VOC contribution to ozone formation [Carter, 1994; DeMore et al., 1997]. The MIR factor scale is used to evaluate the potential contribution of individual VOCs to ozone formation. The ozone formation potential (OFP) represents the maximum ozone concentration generated by these species based on their MIR values. OH radical reactivity is mainly calculated using the propylene-equivalent concentration or the OH consumption rate. Both the MIR factor and OH reactivity methods have advantages and disadvantages [Dimitriades, 1996]. The assessment of OH radical reactivity only considers the kinetic reactivity and fails to notice the difference in the reaction mechanism and reactivity between peroxy radicals and NO. On the other hand, the evaluation of the MIR factor considers the chemical mechanisms and impacts of VOCs/NO*x* ratio on ozone production, however , the MIR factor itself is uncertain and is subject to different chemical mechanisms, local meteorological conditions, and atmospheric composition. Therefore, the MIR factor scale cannot be used alone to assess the effect of VOCs on ozone photochemical formation. In this study, both of the propylene-equivalent concentration method and the OFP method were used to investigate the influence of VOCs in the atmosphere on ozone formation at the monitoring site. The propylene-equivalent concentration (C_{PE} (*i*)) is calculated with the following formula:

$$C_{PE}\ (i) = C_i\ K_{OH}\ (i)/K_{(OH)}(C_3\ H_6) \tag{5}$$

In the formula, *i* represents a certain species of VOC. C_i represents the carbon number concentration (ppbc) contained in the VOC species. K_{OH} (*i*) and K_{OH} (C_3 H_6) represent the chemical reaction rate constants for the reaction of the VOC_i species with OH and propylene radicals, respectively. The reaction rate constants [Atkinson, 1990; Atkinson and Arey, 2003] are shown in Table S2.

The OFP is calculated by weighting the VOC species based on their molecular mass ratio to that of ozone according to the following formula [Ran et al., 2009; Zou et al., 2015; Zou et al., 2021]:

$$OFP\ (i) = MIR \times C\ (ppbv) \times M_i/M_{ozone} \tag{6}$$

M_i and M_{ozone} represent the molecular mass of VOC species *i* and ozone, respectively. C (ppbv) is the measured concentration of VOC species *i*. OFP (*i*) denotes the maximum O_3 concentration that can be formed by VOC species *i*.

It should be noted that early MIR calculations were all based on the 1988 standard scenario (meteorological parameters, emission rate, boundary layer height, and the VOC composition) [Carter, 1994; Carb, 2003; Carter, 2010]. However, Venecek et al. (2018) recently replaced the 1988 scenario with the 2010 scenario to recalculate the MIR factor and found that despite the reduction in the absolute reactivity in the updated 2010 atm, the relative reactivity ranking of VOCs did not change considerably compared to the original 1988 atm. The latest MIR values (g Ozone/g VOCs) according to Venecek et al. (2018) were used in this study, which are shown in Table S2.

2.3.4. Empirical kinetics modeling approach (EKMA)

The results from the Empirical kinetics modeling approach (EKMA) can provide the basis for ozone emission reduction. The hourly observed data of conventional pollutants (O_3, NO*x*, SO_2, CO, etc.), VOCs, and meteorological elements (temperature, pressure, relative humidity, etc.) at the receptor site were used as input for the 0-D observation-based box model based on the Regional Atmospheric Chemical Mechanism (RACM) to describe the nonlinear relationship between ozone and its precursors VOCs and NO*x* together with the EKMA [Zhang et al., 2008; Guo et al., 2017; Liu and Shi, 2021; Guo et al., 2023]. The local ozone

formation regime analysis was carried out by depicting the corresponding ozone formation concentration under different precursor concentration scenarios [Zhang et al., 2008; Guo et al., 2017; Liu and Shi, 2021].

3. Results and discussion

3.1. Calculation of the initial VOC concentrations

The photochemical age method was used to estimate the initial concentration of VOCs in the atmosphere during summer and autumn at the Urban Eco-Meteorological Comprehensive Observation Base in Haizhu District, Guangzhou, as described in Section 2.3.1. Since the main oxidative removal pathway of VOC species is the reaction with OH radicals that occurs during the day [Atkinson and Arey, 2003], this study only estimates the initial concentration of atmospheric VOCs from 7:00 to 18:00. The application of this method requires the selection of appropriate species pairs to estimate the initial concentration of VOCs. This is because the photochemical age of the air mass needs to be characterized by examining the variation in the ratio of specific VOC species pairs. These species pairs should originate from the same source but possess distinct physicochemical properties.

The selected species needs to have a photochemical age that reflects the air mass. In this study, we used the ratio of a reactive VOCs (usually aromatics) to inert acetylene (i.e., ethyne) (Table 1) for judgement and found that the ratios of aromatic hydrocarbon species to ethyne were lower during the daytime than those at night in summer and autumn, which shows clear evidence of photochemical aging. Aromatic hydrocarbon species such as BTEX (benzene, toluene, ethylbenzene, and xylene) can provide evidence for the progress of atmospheric photochemical reactions. Simultaneously, species pairs must have homology, and their respective reaction rates with OH radicals should be different. Linear regression between these aromatic hydrocarbon species can reflect the characteristics of photochemical aging (Table 2). It was found that the concentration of ethylbenzene and *m,p*-xylene was significantly positively correlated in both summer ($R^2 = 0.92$, $p < 0.01$) and autumn ($R^2 = 0.93$, $p < 0.01$), and their reaction rates were reasonably different. The instrument used in this study measures *m*-xylene and *p*-xylene simultaneously, and the derived concentration is the mixture of both species. For this reason, the reaction rate of *m,p*-xylene was calculated as the average reaction rate of *m*-xylene and *p*-xylene, as reported in the literature [Gao et al., 2018; Zou et al., 2021;Wu et al., 2023]. Therefore, ethylbenzene and *m,p*-xylene could be used as suitable species for calculating the initial concentration of VOCs.

In addition, the initial emission ratio of the species pair is an important parameter for the calculation of the initial concentration of VOCs. Based on the selection of ethylbenzene and *m,p*-xylene as the species pair, Fig. 2a and b show the daily variation pattern of the *m,p*-xylene / ethylbenzene ratio in the summer and autumn. As the reaction rate constant of *m,p*-xylene (20.50×10^{-12} molecules^{-1}·cm^3·s^{-1}) with OH radicals during the day was significantly higher than that of ethylbenzene (6.96×10^{-12} molecules^{-1}·cm^3·s^{-1}), the ratio was lower during the day, and it remained constantly high from 20:00 to 6:00. Thus, night time (20:00–6:00) can be considered the period with the weakest photochemical reactions. The maximum ratio between *m,p*-xylene and ethylbenzene in this period can be used as the initial emission ratio of the species pair to estimate the initial concentration of VOC species. Furthermore, through their linear fitting (Fig. 2c and d), their maximum slopes (2.0 ppbv/ppbv and 1.8 ppbv/ppbv) can be selected as their initial emission ratios in the summer and autumn, respectively. In order to validate the accuracy of the initial emission ratio, a comprehensive literature review was conducted. It was found that the initial emission ratio of *m,p*-xylene to ethylbenzene from the main emission sources of VOCs in the PRD region (vehicle emissions and solvent usage) is approximately 2.0 ppbv/ppbv [Liu et al., 2008; Yuan et al., 2010]. Therefore, the initial emission ratio selected in this study is in good agreement with the results of previous studies. Because the analysis of the findings depends on the initial emission ratios, in this study, *m,p*-xylene/ethylbenzene ratios were set to vary within 10 % during both summer and autumn seasons for sensitivity testing to further verify the effectiveness of the estimated initial concentration of VOCs. Based on the sensitivity test, the relative variation of the initial concentration of each VOC species in the summer and autumn ranged from −49.96 % to 47.38 % and from −46.07 % to 56.38 %, respectively.

Overall, the estimation of the initial VOC concentration is highly dependent on the selection of the initial emission ratio and species pair, which is also an important reason for the uncertainty of the estimation. In addition, the reaction rates of VOCs and OH radicals used in the calculation are based on the work of Atkinson and Arey (2003) at a K*i* value of 298 K (i.e., 24.85 °C). However, the observed average temperature during the daytime in the summer and autumn was 30.84 °C and 27.55 °C respectively, introducing some uncertainty to the calculation results of the initial VOC concentration in the actual scenario. When toluene/benzene and *o*-xylene/toluene were used to calculate the reaction rates of all major anthropogenic VOC species with OH radicals, the estimation of the initial concentrations fluctuated greatly and deviated significantly from the average (e.g., alkenes) as shown by de Gouw et al. (2005). Therefore, in this study, the reaction rate of *m,p*-xylene was uniformly adopted for VOC species with reaction rates higher than *m,p*-xylene, rather than using the rate itself, which would lead to an underestimation of the initial concentration of VOCs.

Table 1
Ratios between Benzene (B), Toluene (T), Ethylbenzene (E), *m,p*-Xylene (M,P), and o-xylene (O) and ethyne (e) during the daytime (D) and nightime (N) in summer and autumn.

	B/e	T/e	E/e	M,P/e	O/e
Obs-D(Summer)	0.55	1.69	0.38	0.53	0.37
Obs-N(Summer)	0.56	2.23	0.50	0.87	0.56
Obs-D(Autumn)	0.26	0.88	0.19	0.23	0.20
Obs-N(Autumn)	0.27	1.03	0.23	0.35	0.28

Table 2
Linear relationship between aromatic hydrocarbons in summer and autumn.

	Benzene	Toluene	Ethylbenze	*M,P*-Xylene
Summer				
Benzene	1			
Toluene	0.07	1		
Ethylbenzene	0.06	0.60	1	
M,P-Xylene	0.06	0.70	0.92	1
O-Xylene	0.06	0.47	0.63	0.72
Autumn				
Benzene	1			
Toluene	0.12	1		
Ethylbenzene	0.09	0.65	1	
M,P-Xylene	0.10	0.63	0.93	1
O-Xylene	0.08	0.62	0.93	0.98

3.2. Characterization of VOCs based on photochemical loss

Fig. 3 shows the observed concentration in daytime (Obs—D), initial concentration in daytime (Ini—D), and observed concentration at nighttime (Obs—N) of VOC components in the summer and autumn at the Urban Eco-Meteorological Comprehensive Observation Base in Haizhu District, Guangzhou. In both summer and autumn, alkanes were the most abundant VOCs in the Obs-D and Ini—D, accounting for over 50 % of the total target VOCs, followed by aromatics and alkenes, with acetylene contributing the least. The photochemical age method estimated the initial concentrations of VOCs to be 32.32 ppbv and 25.51 ppbv in summer and autumn, respectively, which were 5.12 ppbv and

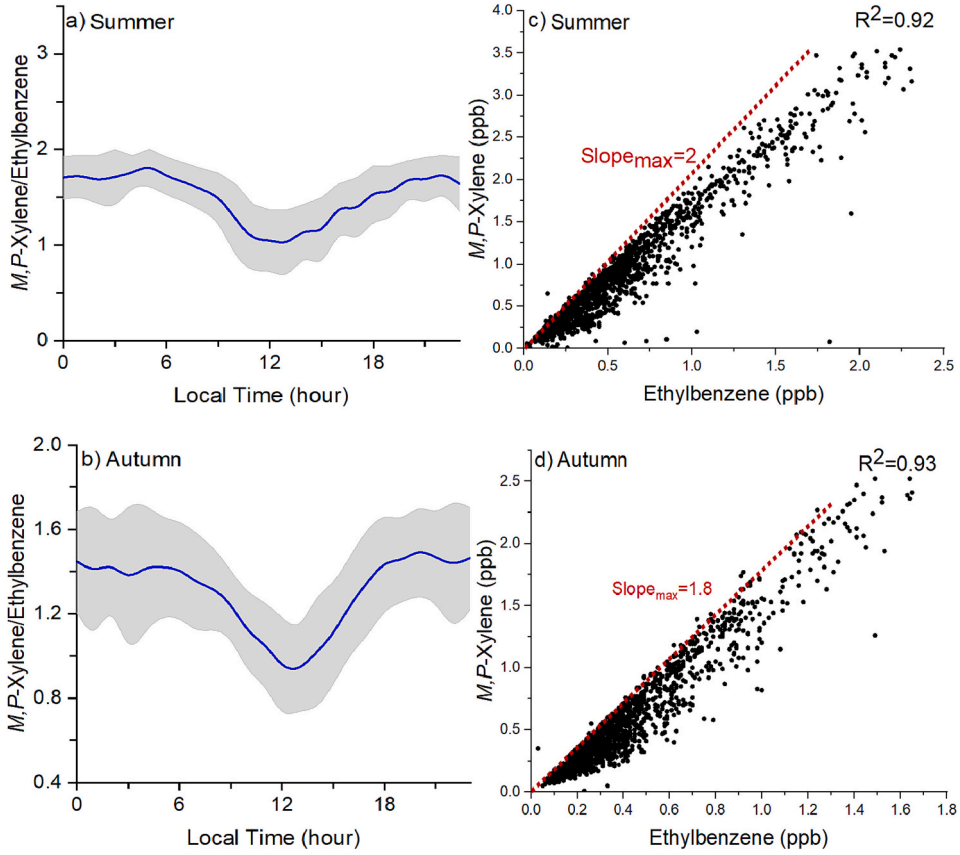

Fig. 2. (a,b) Diurnal variation and (c, d) scatter plot of *m,p*-xylene/ethylbenzene during summer and autumn.

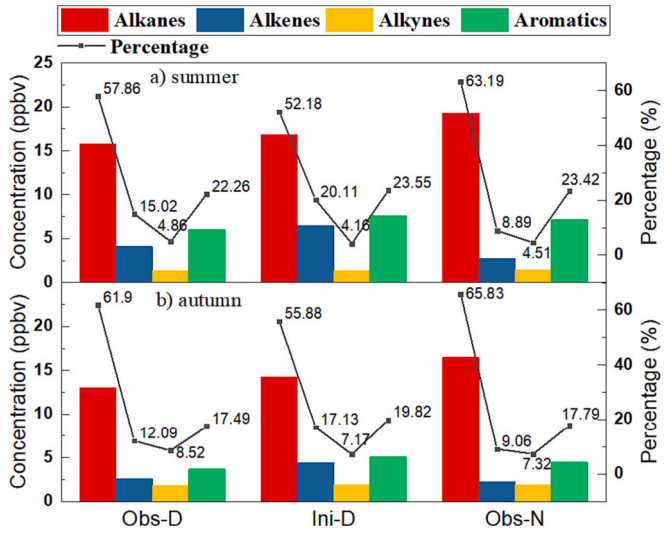

Fig. 3. The daytime observed (Obs—D), daytime initial (Ini—D), and nighttime observed (Obs—N) concentration and relative contributions of alkanes, alkenes, alkynes and aromatics in the summer and autumn.

4.49 ppbv higher than the observed concentrations. Although the absolute VOC loss in summer was higher than in autumn, the VOC loss rate in summer (15.8 %) was lower than in autumn (17.6 %). This may be due to lower boundary layer height (BLH) or lower wind speed in autumn compared to summer. Alkenes exhibited the highest absolute loss among the VOC categories, with initial concentrations 2.42 ppbv and 1.83 ppbv higher than measured concentrations in summer and autumn, respectively. Moreover, alkenes showed a significant increase in the relative contribution to chemical loss during both summer (5.09 %) and autumn (5.04 %). This indicates their higher chemical reactivity, as they quickly react with OH radicals and are consumed at a faster rate during the daytime. Similarly, aromatics showed strong atmospheric chemical activity, with initial concentrations 1.56 ppbv and 1.38 ppbv higher than measured concentrations in summer and autumn, respectively. The relative contributions of the chemical mixing ratio loss for aromatics increased by 1.29 % and 2.33 % in summer and autumn, respectively. In contrast, the chemical loss concentrations of alkanes and alkynes were lower than those of alkenes and aromatics due to their lower atmospheric chemical activities. Consequently, their relatively smaller contributions to the chemical loss concentration decreased in summer and autumn. Furthermore, the observed daytime VOC concentrations in summer and autumn were lower than the nighttime concentrations (3.35 ppbv and 4.00 ppbv lower, respectively). Although VOC emissions from solvent evaporation and biogenic sources were stronger during the day, higher nighttime concentrations were expected due to photochemical loss during the daytime and the lower temperature and boundary layer height at night, which are more conducive to VOC accumulation.

3.3. Source apportionment considering the photochemical loss of VOCs

The conventional PMF receptor model method does not take into account the impact of atmospheric photochemical reactions on the concentration and composition of VOCs during their transport from emission sources to the receptor site. This omission can introduce deviations in accurately identifying and characterizing VOC sources. In this study, the initial concentrations of VOC species estimated in Section 3.2 were used as environmental data input for the PMF5.0 model developed by the US-EPA to analyze the sources of VOCs in the actual environment. The results were compared with traditional PMF source

contribution results based on observation data from the monitoring site to explore the influence of atmospheric photochemical reactions on the VOC source analysis. The PMF model identified five potential sources of VOCs in both the summer and autumn seasons based on the initial concentration of VOCs. Notably, the factors resolved by the PMF model differed between the two seasons due to variations in the emission characteristics of VOCs. While the sources of LPG usage + vehicle emissions and gasoline evaporation (summer) were slightly different from the sources of LPG usage + gasoline evaporation and vehicle emissions (in the autumn), the remaining identified sources were the same, which included biogenic emissions, solvent usage, and industrial emissions (Fig. 4). In the summer, Factor 1 mainly contained LPG tracers propane and *n*-/*i*-butane (62.97 %) [Guo et al., 2004] and tracers of vehicle exhaust ethane, ethylene, and acetylene (30.33 %) [Guo et al., 2004, 2011a, 2011b] representing a mixture of LPG usage + vehicle emissions as this factor does not contain benzene series. Factor 2 was

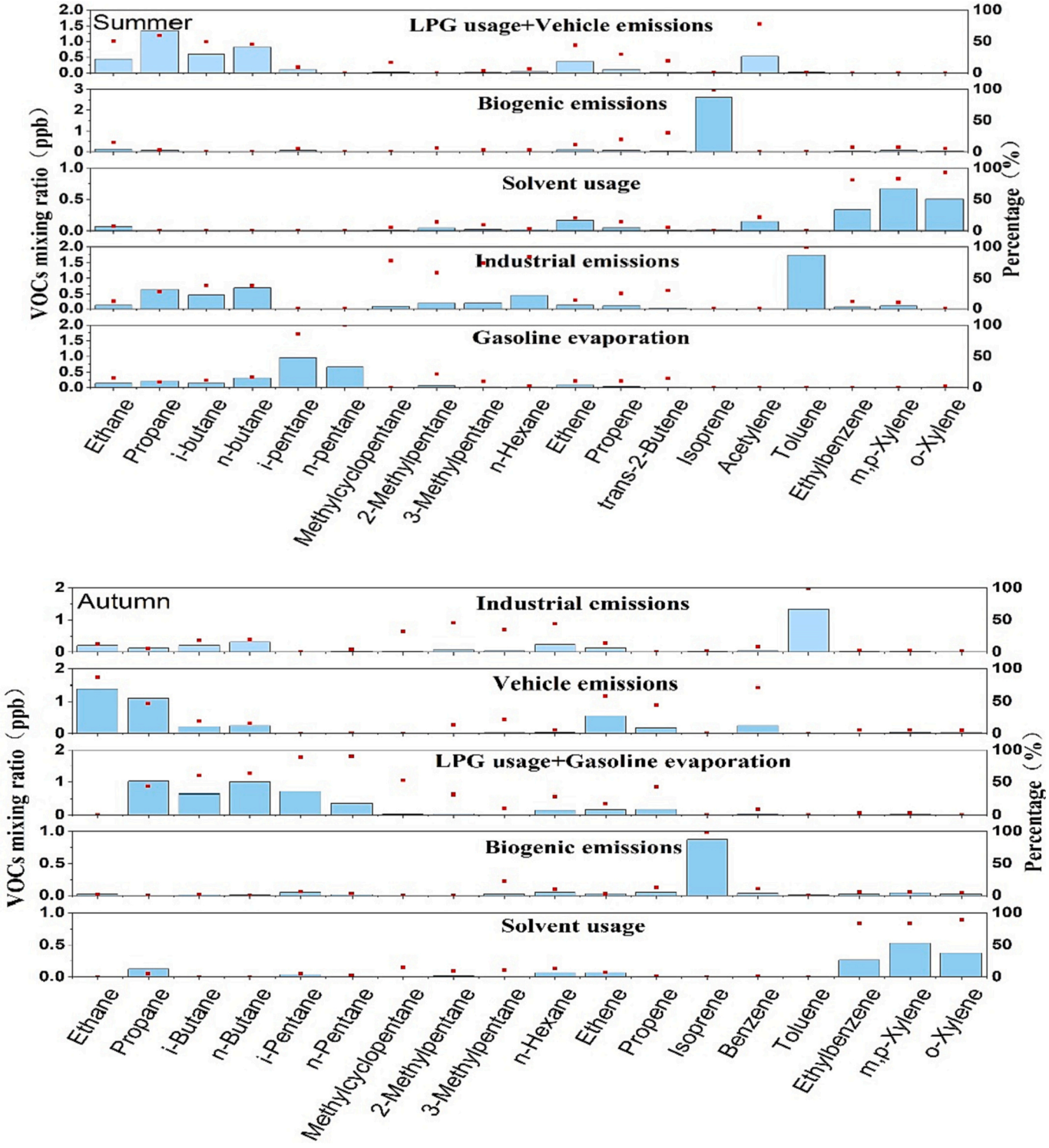

Fig. 4. VOC source profiles by PMF model considering chemical loss in summer (top) and autumn (bottom). The bars represent the mixing ratio of species. The red dots represent the percent contribution of the species to the factor.

dominated by isoprene (81.34 %), a typical biogenic VOC [Guo et al., 2007; Zou et al., 2019b, 2021]. Factor 3 consisted of ethylbenzene, *m,p*-xylene, and o-xylene in the benzene series (74.12 %), related to solvent usage such as paints and coatings [Guo et al., 2004, 2007; Ling et al., 2011]. Factor 4 represented an industrial source with high levels of toluene (35.79 %) and small amounts of propane, *n*-/*i*-butane, and *n*-hexane [Liu et al., 2008; Wang et al., 2023]. Factor 5 was related to gasoline evaporation, with *n*-/*i*-pentane accounting for a high proportion of 61.06 % [Tsai et al., 2006; Liu et al., 2017]. In the autumn, Factor 1 had a higher proportion of toluene (49.34 %), similar to Factor 4 in the summer, defining it as an industrial source. Factor 1 also contained higher levels of ethane and ethylene (47.67 %), and a relatively small amount of *n*-/*i*-butane used in LPG led to its identification as vehicle emissions. Factor 3 included typical LPG component markers propane and *n*-/*i*-butane (61.25 %) and *n*-/*i*-pentane (39.40 %), related to gasoline evaporation, leading to its identification as LPG usage + gasoline evaporation. Factor 4 was dominated by natural source marker isoprene (70.62 %), indicating biogenic emissions. Factor 5, similar to Factor 3 in the summer, consisted of ethylbenzene, *m,p*-xylene, and *o*-xylene (77.22 %), categorized as solvent usage.

Regarding the emission contributions of each source, as depicted in Fig. 5, the PMF method was used for both measured and initial VOCs. It was observed that LPG usage, vehicle emissions, and gasoline evaporation sources are responsible for emitting significant amounts of low-activity alkane species, such as propane, *n*−/*i*-butane, and *n*-/*i*-pentane. These alkane species exhibit lower levels of chemical reactivity, resulting in relatively lower rates of consumption or loss in the atmosphere. Consequently, the contributions of these sources based on measured concentrations are often relatively overestimated because these sources predominantly emit low-activity alkane species which have lower rates of chemical loss during transport. On the other hand, solvent usage and industrial emissions are associated with high-activity aromatics species like toluene, ethylbenzene, and xylene, which undergo significant chemical loss during transport. Hence, the contributions of solvent usage, industrial emissions, and biogenic sources, characterized by highly reactive species like isoprene, are underestimated based on measured concentrations. These observations are consistent with the findings reported by Wu et al. (2023). Specifically, in the summer, LPG usage + vehicle emissions and gasoline evaporation, based on PMF analysis of the observed concentrations of VOCs, increased by approximately 1.33 % and 1.45 %, respectively, compared to the contribution calculated based on initial concentrations. In contrast, the relative contribution ratios of biogenic source emissions and solvent usage decreased by 4.58 % and 0.75 %, respectively. In the autumn, LPG usage + gasoline evaporation and vehicle emissions, based on the PMF analysis of the observed concentrations of VOCs, increased by 3.92 % and 4.35 %, respectively, compared to the initial concentration-based contribution ratio. At the same time, the relative contribution ratios of biogenic source emissions and solvent usage decreased by 3.13 % and 1.45 %, respectively.

3.4. The effect of VOCs on ozone formation based on photochemical loss

The traditional method used to evaluate the impact of VOCs on ozone formation does not take into account their chemical loss, leading to an underestimation of their actual effects on ozone formation. Based on the estimates of the initial concentrations of VOC species in the previous section, this study uses the propylene-equivalent concentration method and OFP method to calculate the VOCs' contribution to ozone formation and compares this approach to the traditional method based on observation data collected at the monitoring site. The effect of atmospheric photochemical reactions of VOCs on ozone formation was explored. As shown in Fig. 6, the ozone formation contribution estimated by the OFP method and propylene-equivalent concentration method based on the initial concentration in the summer is 53.24 ppbv and 47.25 ppbc higher than those of the traditional method based on observational data, respectively, with the largest loss of alkenes components (30.18 ppbv and 35.75 ppbc, respectively). In the autumn, the levels are higher than summer with 40.34 ppbv and 26.37 ppbc, respectively, and the loss of alkenes components is the greatest (19.76 ppbv and 16.22 ppbc, respectively). This shows that the evaluation of ozone formation without the consideration of atmospheric photochemical loss is underestimated, especially for chemically active components. During the summer season, when the OFP and propylene-equivalent concentration methods were used to evaluate the contribution of VOCs to ozone formation based on the initial concentration of VOCs, we observed that alkenes (40.64 % and 64.43 %) and aromatics (42.30 % and 24.57 %) had the highest contributions. In the autumn, alkenes and aromatic hydrocarbons

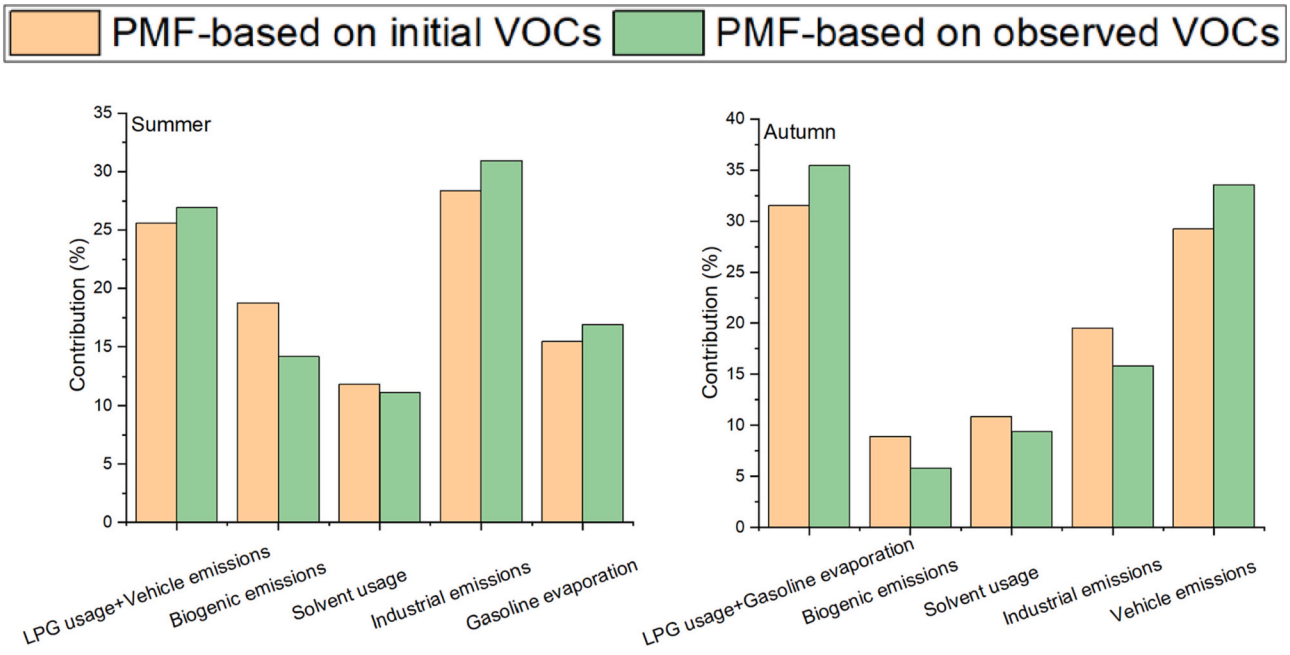

Fig. 5. Source contributions by PMF model using the initial and observed VOCs during summer (left) and autumn (right).

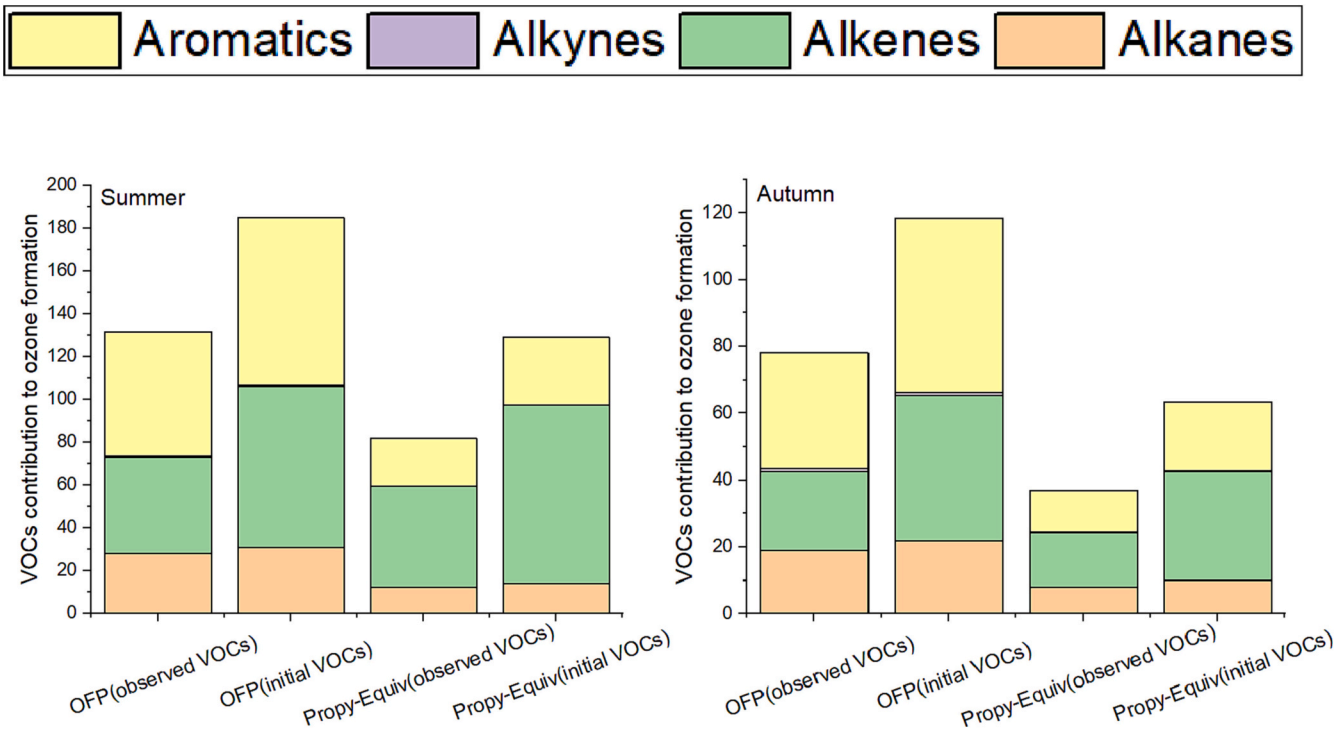

Fig. 6. The OFP (ppbv) and Propy-Equiv (ppbc) concentrations of VOC components using the observed and initial concentrations during the summer (left) and autumn(right).

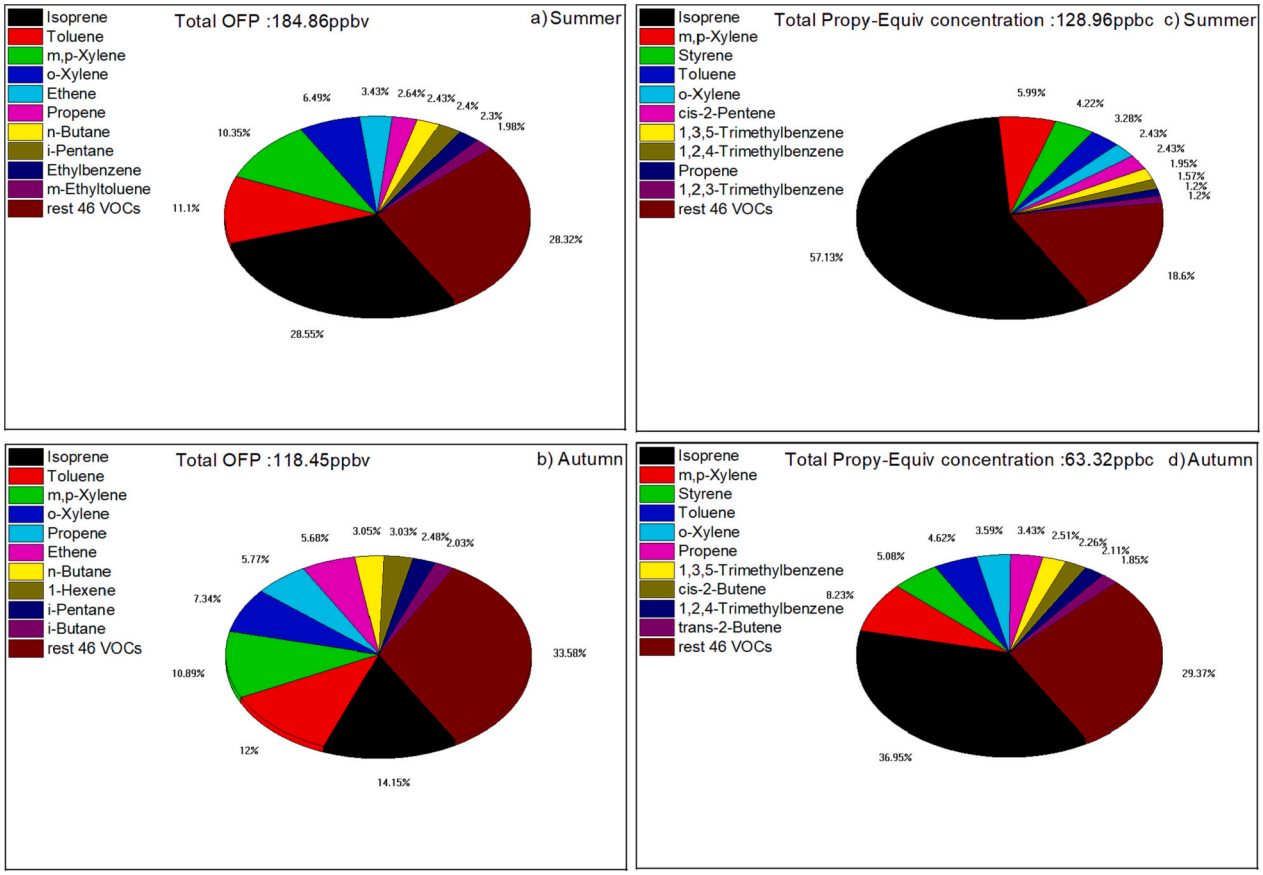

Fig. 7. The relative contribution of VOCs by (a,b) OFP method and (c,d) propylene-equivalent concentration method in summer and autumn.

accounted for 36.51 % and 51.53 %, and 44.16 % and 32.59 %, according to the OFP and propylene-equivalent concentration methods, respectively. The propylene-equivalent concentration method (which only considers kinetic activity) may overestimate species with fast OH reaction rates (such as isoprene) when evaluating the contributions of VOCs to ozone formation because it ignores the mechanistic activity difference between peroxy radicals and NO reactions, leading to an increase in the proportion of alkenes. As shown in Fig. 7, the OFP and propylene-equivalent concentration methods were used to compare and analyze the top 10 VOC species contributing to ozone in the summer and autumn based on the initial concentration of VOCs. Half of the species were found to be identical. In particular, the descriptions of the species that have higher contributions to ozone formation were consistent: isoprene, toluene, and xylene were the species that contributed the most to ozone formation. They accounted for 56.49 % of OFP and 68.83 % of the total propylene-equivalent concentration in the summer, while in the autumn, they accounted for 44.38 % of OFP and 53.39 % of the total propylene-equivalent concentration. Overall, we found that these two methods may fairly reflect the ozone formation contribution of the VOC species.

In addition, to investigate the impact of atmospheric chemical loss on the mechanism of ozone formation, an observation-based box model was employed. Through this approach, the nonlinear relationship between VOCs, NO*x*, and O_3 was examined by plotting the empirical kinetics modeling approach (EKMA) curve. We calculated the hourly mean of VOCs, NO*x*, SO_2, CO, temperature, pressure, and relative humidity from each day of summer and autumn as the initial conditions to drive the box model. We conducted 102 and 126 scenarios in summer and autumn, respectively, and simulated the entire episode to analyze the daily maximum 1-h average concentration. As shown in Fig. 8, the ozone formation regime is divided into three parts according to the ridge (dotted) line: (1) the upper-left panel is the VOC-limited regime, (2) the lower-right panel is the NO*x*-limited regime, and (3) the area near the ridge line between the upper-left and lower-right is considered the VOC-NO*x* transition regime. Most of the observational data (left figures) for the summer and autumn are in the VOC-limited regime. When considering atmospheric chemical loss (right figures), the initial VOC concentration data for the summer are near the VOC-NO*x* transition regime, thus, ozone formation shifts from the VOC-limited regime to the VOC-NO*x* transition regime. In the autumn, ozone formation moves from the relatively strong VOC-limited regime (i.e., the data points are closer to the ridge of the EKMA curve) to the relatively weak VOC-limited regime (i.e., the data points are further away from the ridge of the EKMA curve), and VOC control declines in both the summer and autumn in the ozone formation regime. Since VOCs undergo a series of photochemical loss, and ozone formation is closely associated with the loss of VOCs, an assessment of the ozone formation regime that considers the chemical loss of VOCs is more reasonable. However, further research is needed to draw more detailed and reliable conclusions on this basis. It should be noted that, as mentioned above, firstly, due to the use of molybdenum converters in the measurement phase of NO*x*, the measured NO*x* may include some oxidized reactive nitrogen, causing its measured value to be higher than the actual value, which may also introduce bias into the evaluation of the ozone formation regime. Secondly, this study considers the reaction with OH radicals, which may result in lower VOCs chemical losses compared to the actual values. Furthermore, when the reaction rates of VOC species were higher than *m,p*-xylene, the study uniformly adopted the reaction rates of *m,p*-xylene. This could potentially lead to an underestimation of VOCs loss. As a result, these factors may introduce bias into the evaluation of the ozone formation regime, which tends to

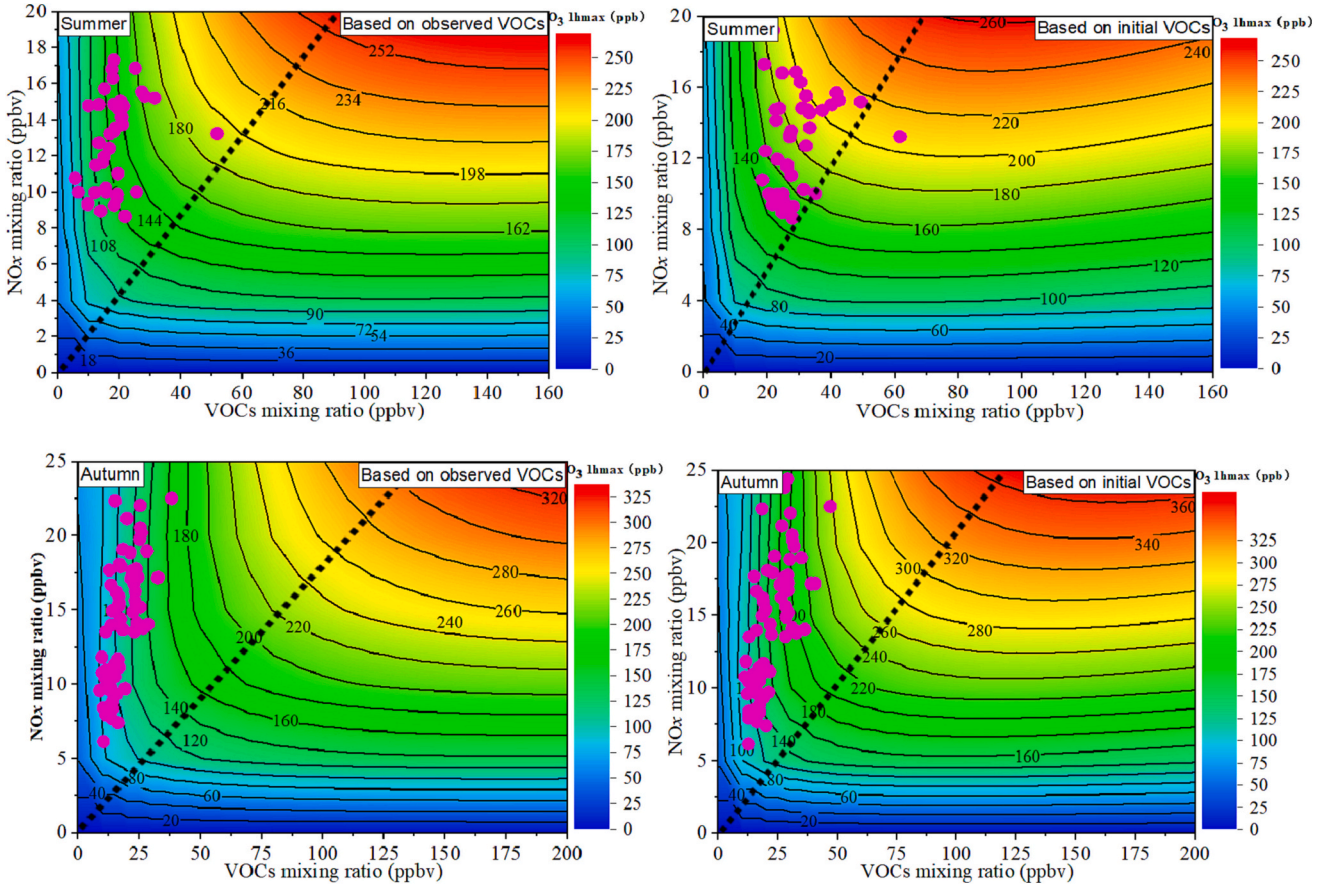

Fig. 8. The model simulated daily $O_{3\ 1h\ max}$ isopleth diagram of observed or initial VOCs and NO*x* during summer and autumn. Colored dots represent the scatter of VOCs and NO*x* in each day.

be inclined to the NO*x*-limited transition.

4. Conclusions

In this study, an online monitoring campaign was conducted at the Urban Eco-Meteorological Comprehensive Observation Base in Guangzhou during the summer and autumn of 2021. The focus was on VOCs and meteorological conditions. The initial concentration of VOCs was estimated using the photochemical age method. It was found that while the absolute loss of VOCs in summer (5.12 ppbv) was relatively higher than in autumn (4.49 ppbv), the loss rate in summer (15.8 %) was lower than in autumn (17.6 %). Alkenes and aromatics showed significant atmospheric chemical activity, resulting in higher chemical loss within the VOCs categories. We found that not considering the chemical reaction of VOC species in the source-receptor process could lead to differences in the contribution from various sources. Industrial emissions, solvent usage, and biogenic sources emitted relatively reactive VOCs species (i.e., alkenes and aromatics), resulting in significant consumption during transport, leading to an underestimation of their contribution based on measured concentrations. On the other hand, LPG usage, vehicle emissions, and gasoline evaporation were associated with relatively inactivity VOC species (i.e., alkanes), which experience less chemical loss during transport, resulting in an overestimation based on measured concentrations. The evaluation of the effect of VOCs on ozone formation contribution using the OFP and propylene-equivalent concentration methods without considering atmospheric photochemical loss underestimated the contribution in both summer and autumn by 53.24 ppbv and 47.25 ppbc in the summer, respectively, and 40.34 ppbv and 26.37 ppbc, in the autumn, respectively. Because the species that have higher contributions to ozone formation showed consistent results when analyzed using both the OFP and propylene-equivalent concentration methods, employing these two methods can effectively reflect the ozone formation contributions of the VOC species. Moreover, when atmospheric chemical loss was considered, the VOC control demonstrated reductions in ozone formation during both summer and autumn seasons.

CRediT authorship contribution statement

Y. Zou: Conceptualization, Methodology, Formal analysis, Writing – original draft, Writing – review & editing. **X.L. Yan:** Methodology, Software. **R.M. Flores:** Validation, Writing – review & editing. **L.Y. Zhang:** Investigation. **S.P. Yang:** Investigation. **L.Y. Fan:** Validation. **T. Deng:** Validation. **X.J. Deng:** Validation. **D.Q. Ye:** Supervision.

Declaration of competing interest

The authors declare that they have no known competing financial interests or personal relationships that could have appeared to influence the work reported in this paper.

Data availability

The authors do not have permission to share data.

Acknowledgements

This work was supported by the Key Area Research and Development Program of Guangdong Province (2020B1111360003), Guangdong Basic and Applied Basic Research Foundation (2023A1515012205, 2023A1515012448, 2022A1515011753), the National Natural Science Foundation of China (42275123, 42275093, 41905123), the Technology Innovation Team Plan of Guangdong Meteorological Bureau (GRMCTD202003) and the Science and Technology Research project of Guangdong Meteorological Bureau (GRMC2021Q02, GRMC2020Z06). We would like to extend our sincerest appreciation to Dr. Kathy M. Krause for her invaluable contribution in proofreading our manuscript.

Appendix A. Supplementary data

Supplementary data to this article can be found online at https://doi.org/10.1016/j.scitotenv.2023.166191.

References

Atkinson, R., 1990. Gas-phase tropospheric chemistry of organic compounds: a review. Atmos. Environ. 24A, 1–41.
Atkinson, R., Arey, J., 2003. Atmospheric degradation of volatile organic compounds. Chem. Rev. 103, 4605–4638.
Bertman, S.B., Roberts, J.M., Parrish, D.D., et al., 1995. Evolution of alkyl nitrates with air mass age. J. Geophys. Res. Atmos. 100 (D11), 22805–22814.
Bon, D.M., Ulbrich, I.M., Kuster, W.C., et al., 2011. Measurements of volatile organic compounds at a suburban ground site (T1) in Mexico City during the MILAGRO 2006 campaign: measurement comparison, emission ratios, and source attribution. Atmos. Chem. Phys. 11, 2399–2421.
CARB, 2003. Rulemaking on the Adoption of Proposed Amendments to the Tables of Maximum Incremental Reactivity (MIR) Values, California Air Resources Board, December3. Available at. http://www.arb.ca.gov/regact/mir2003/mir2003.htm. Accessed August 14, 2009. Document giving MIR values is available at http://www.arb.ca.gov/regact/mir2003/fsor.doc.
Carter, W.P.L., 1994. Development of ozone reactivity scales for volatile organic compounds. J. Air Waste Manage. Assoc. 44, 881–899.
Carter, W.P.L., 2010. Development of the SAPRC-07 chemical mechanism. Atmos. Environ. 44 (40), 5324–5335.
de Gouw, J.A., Middlebrook, A.M., Warneke, C., 2005. Budget of organic carbon in a polluted atmosphere: results from the New England air quality study in 2002. J. Geophys. Res. 110, D16305.
DeMore, W.B., Sander, S.P., Golden, D.M., et al., 1997. Chemical Kinetics and Photochemical Data for Use in Stratospheric Modeling: Evaluation Number 12. Jet Propulsion Laboratory Publication, NASA, 97-4.
Dimitriades, B., 1996. Scientific basis for the VOC reactivity issues raised by section 183 (e) of the clean air act amendments of 1990. J. Air Waste Manage. Assoc. 46, 963–970.
Dunlea, E.J., Herndon, S.C., Nelson, D.D., et al., 2007. Evaluation of nitrogen dioxide chemilumines-cence monitors in a polluted urban environment. Atmos. Chem. Phys. 7, 2691–2704.
Gao, J., Zhang, J., Li, H., et al., 2018. Comparative study of volatile organic compounds in ambient air using observed mixing ratios and initial mixing ratios taking chemical loss into account-a case study in a typical urban area in Beijing. Sci. Total Environ. 628-629, 791–804.
Gao, Y., Li, M., Wan, X., et al., 2021. Important contributions of alkenes and aromatics to VOCs emissions, chemistry and secondary pollutants formation at an industrial site of central eastern China. Atmos. Environ. 244, 117927.
GB 3095-2012, 2012. Ambient Air Quality Standards. Ministry of Environmental Protection, Beijing, China.
Guo, H., Wang, T., Louie, P.K.K., 2004. Source apportionment of ambient non-methane hydrocarbons in Hong Kong: application of a principal component analysis/absolute principal component scores (PCA/APCS) receptor model. Environ. Pollut. 129, 489–498.
Guo, H., So, K.L., Simpson, I.J., et al., 2007. C_1-C_8 volatile organic compounds in the atmosphere of Hong Kong: overview of atmospheric processing and source apportionment. Atmos. Environ. 41, 1456–1472.
Guo, H., Cheng, H.R., Ling, Z.H., et al., 2011a. Which emission sources are responsible for the volatile organic compounds in the atmosphere of Pearl River Delta? J. Hazard. Mater. 188, 116–124.
Guo, H., Zou, S.C., Tsai, W.Y., et al., 2011b. Emission characteristics of nonmethane hydrocarbons from private cars and taxis at different driving speeds in Hong Kong. Atmos. Environ. 45 (16), 2711–2721.
Guo, H., Ling, Z.H., Cheng, H.R., et al., 2017. Tropospheric volatile organic compounds in China. Sci. Total Environ. 54, 1021–1043.
Guo, J., Zhang, X.S., Gao, Y., et al., 2023. Evolution of ozone pollution in China: what track will it follow? Environ. Sci. Technol. 57, 109–117.
Li, X.B., Yuan, B., David, D.P., et al., 2022. Long-term trend of ozone in southern China reveals future mitigation strategy for air pollution. Atmos. Environ. 269, 118869.
Ling, Z.H., Guo, H., Cheng, H.R., 2011. Sources of ambient volatile organic compounds and their contributions to photochemical ozone formation at a site in the Pearl River Delta, southern China. Environ. Pollut. 159, 2310–2319.
Liu, C., Shi, K., 2021. A review on methodology in O_3-NOx-VOC sensitivity study. Environ. Pollut. 291, 118249.
Liu, Y., Shao, M., Fu, L.L., et al., 2008. Source profiles of volatile organic compounds (VOCs) measured in China: part I. Atmos. Environ. 42, 6247–6260.
Liu, C.T., Ma, Z.B., Mu, Y.J., et al., 2017. The levels, variation characteristics, and sources of atmospheric non-methane hydrocarbon compounds during wintertime in Beijing, China. Atmos. Chem. Phys. 17, 10633–10649.
Main, H.H., Roberts, P.T., Hurwitt, S.B., 1999. Validation of PAMS VOC Data in the Mid-Atlantic Region. Report Prepared for MARAMA, Baltimore, MD. Sonoma technology, Inc., Petaluma. CA STI-998481-1835-FR.
McKeen, S.A., Liu, S.C., Hsie, E.Y., et al., 1996. Hydrocarbon ratios during PEM-WEST A: a model perspective. J. Geophys. Res. 101, 2087–2109.

Meng, X., Jiang, J.K., Chen, T.S., et al., 2023. Chemical drivers of ozone change in extreme temperatures in eastern China. Sci. Total Environ. 874, 162424.
Mu, J.S., Zhang, Y.N., Xia, Z.Y., et al., 2023. Two-year online measurements of volatile organic compounds (VOCs) at four sites in a Chinese city: significant impact of petrochemical industry. Sci. Total Environ. 858, 159951.
Na, K.S., Kim, Y.P., 2007. Chemical mass balance receptor model applied to ambient C_2-C_9 VOC concentration in Seoul, Korea: effect of chemical reaction losses. Atmos. Environ. 41 (32), 6715–6728.
Parrish, D.D., Stohl, A., Forster, C., et al., 2007. The effects of mixing on evolution of hydrocarbon ratios in the troposphere. J. Geophys. Res. Atmos. 112 (D10), D10S34.
Ran, L., Zhao, C.S., Geng, F.H., 2009. Ozone photochemical production in urban Shanghai, China: analysis based on ground level observations. J. Geophys. Res. 114, D15301.
Ran, L., Zhao, C.S., Xu, W.Y., et al., 2011. VOC reactivity and its effect on ozone production during the HaChi summer campaign. Atmos. Chem. Phys. 11, 4657–4667.
Shao, M., Lu, S.H., Liu, Y., 2009. Volatile organic compounds measured in summer in Beijing and their role in ground-level ozone formation. J. Geophys. Res. Atmos. 114, D00G06.
Shao, M., Wang, B., Lu, S.H., et al., 2011. Effects of Beijing Olympic control measures of reducing reactive hydrocarbon species. Environ. Sci. Technol. 45, 514–519.
Shiu, C.J., Liu, S.C., Chang, C.C., et al., 2007. Photochemical production of ozone and control strategy for southern Taiwan. Atmos. Environ. 41, 9324–9340.
Song, K.X., Liu, R., Wang, Y., et al., 2022. Observation-based analysis of ozone production sensitivity for two persistent ozone episodes in Guangdong, China. Atmos. Chem. Phys. 22, 8403–8416.
Tsai, W.Y., Chan, L.Y., Blake, D.R., et al., 2006. Vehicular fuel composition and atmospheric emissions in South China: Hong Kong, Macau, Guangzhou, and Zhuhai. Atmos. Chem. Phys. 6, 3281–3288.
USEPA, 2014. Epa Positive Matrix Factorization (PMF) 5.0 Fundamentals & User Guide. USEPA Office of Research and Development.
Venecek, M.A., Carter, W.P.L., Kleeman, M.J., 2018. Updating the SAPRC maximum incremental reactivity (MIR) scale for the United States from 1988 to 2010. J. Air Waste Manag. Assoc. 2162–2906.
Wang, H.L., Chen, C.H., Wang, Q., et al., 2013. Chemical loss of volatile organic compounds and its impact on the source analysis through a two-year continuous measurement. Atmos. Environ. 80, 488–498.
Wang, N., Xu, J.W., Pei, C.L., et al., 2021. Air quality during COVID-19 lockdown in the Yangtze River and the Pearl River Delta: two different responsive mechanisms to emission reductions in China. Environ. Sci. Technol. 55, 5721–5730.
Wang, W.J., Parrish, D.D., Wang, S.W., et al., 2022. Long-term trend of ozone pollution in China during 2014-2020: distinct seasonal and spatial characteristics and ozone sensitivity. Atmos. Chem. Phys. 22, 8935–8949.
Wang, B.L., Liu, Z.G., Li, Z.A., et al., 2023. Characteristics, chemical transformation and source apportionment of volatile organic compounds (VOCs) during wintertime at a suburban site in a provincial capital city, east China. Atmos. Environ. 298, 119621.
Warneke, C., Mckeen, S.A., de Gouw, J.A., et al., 2007. Determination of urban volatile organic compound emission ratios and comparison with an emissions database. J. Geophys. Res. Atmos. 112 (D10), D10S47.
Wu, Y.J., Fan, X.L., Liu, Y., et al., 2023. Souce apportionment of VOCs based on photochemical loss in summer at a suburban site in Beijing. Atmos. Environ. 293, 119459.
Yang, X.P., Lu, K.D., Ma, X.F., et al., 2021. Observations and modeling of OH and HO_2 radicals in Chengdu, China in summer 2019. Sci. Total Environ. 772, 144829.
Yin, C.Q., Deng, X.J., Zou, Y., et al., 2019. Trend analysis of surface ozone at suburban Guangzhou, China. Sci. Total Environ. 695, 133880.
Yuan, B., Shao, M., Lu, S.H., et al., 2010. Source profiles of volatile organic compounds associated with solvent use in Beijing, China. Atmos. Environ. 44, 1919–1926.
Zhan, J.L., Feng, Z.M., Liu, P.F., et al., 2021. Ozone and SOA formation potential based on photochemical loss of VOCs during the Beijing summer. Environ. Poll. 285, 117444.
Zhang, Y.H., Su, H., Zhong, L.J., et al., 2008. Regional ozone pollution and observation-based approach for analyzing ozone-precursor relationship during the PRIDE-PRD2004 campaign. Atmos. Environ. 42, 6203–6218.
Zou, Y., Deng, X.J., Zhu, D., et al., 2015. Characteristics of 1 year of observational data of VOCs, NOx and O_3 at a suburban site in Guangzhou, China. Atmos. Chem. Phys. 15, 6625–6636.
Zou, Y., Charlesworth, E., Yin, C.Q., et al., 2019a. The weekday/weekend ozone differences induced by the emissions change during summer and autumn in Guangzhou, China. Atmos. Environ. 199, 114–126.
Zou, Y., Deng, X.J., Deng, T., et al., 2019b. One-year characterization and reactivity of isoprene and its impact on surface ozone formation at a suburban site in Guangzhou, China. Atmosphere 10, 201.
Zou, Y., Charlesworth, E., Wang, N., et al., 2021. Characterization and ozone formation potential (OFP) of non-methane hydrocarbons under the condition of chemical loss in Guangzhou, China. Atmos. Environ. 262, 118630.